F. H. Cornet

Laboratoire d'Etude Géophysique
des Structures Profondes,
Institut de Physique
du Globe de Paris,
Université Paris VI,
4 Place Jussieu,
Paris 75230, France

Comparative Analysis by the Displacement-Discontinuity Method of Two Energy Criteria of Fracture

This paper discusses the applicability of the displacement-discontinuity technique to crack propagation analysis for plane strain conditions. Results derived from the maximum strain-energy release-rate hypothesis are compared to those obtained with the critical strain-energy-density-factor theory. It is shown that for tensile stress fields both theories give similar results but that they differ for compressive stress fields. Experimental results are more in support of the maximum strain-energy release-rate model.

Introduction

Although a few attempts have been made to derive stress criteria of fracture for homogeneous materials by correlating the cohesive force between atoms to fracture resistance, no satisfactory criterion has yet been proposed. Even if such a relationship could be defined its applicability to fracture of very heterogeneous materials like rocks would be extremely doubtful since an exact stress field characterization cannot be derived with this type of material. Yet rock fracture occurs and it is necessary to develop a theory which represents satisfactorily the features associated with this fracturing process.

The present paper describes a numerical technique for determining the path of fissures when fracture develops in linearly elastic homogeneous isotropic solids subjected to quasi-static plane strain conditions. Although this model cannot be applied in a straightforward manner to rocks, it sheds light on some basic mechanisms inherent to fracture development in compressive stress fields.

First, two possible energy criteria of failure are considered; namely, the maximum strain-energy release rate [1, 2] and the critical strain-energy-density factor [3]. Then the numerical technique which is derived from the displacement-discontinuity method proposed by

Crouch [4], is briefly described. Finally, practical examples are considered and the results from the two criteria are compared.

Fracture Criteria and Stability Analysis

Griffith [1] derived a fracture criterion from the theorem of minimum potential energy on the assumption that extension of a fractured surface absorbs an amount of energy directly proportional to the area of these new surfaces.

If γ is the surface energy of the material, this fracture criterion can be expressed by the following equations:

$$dW_E(\mathbf{ds}) \geq dW_B(\mathbf{ds}) \tag{1}$$

$$dW_B(\mathbf{ds}) = \gamma da \tag{2}$$

where $dW_E(\mathbf{ds})$ is the quantity of strain energy released by the formation of new surface element $\mathbf{ds} = \mathbf{n}da$ ($\mathbf{n}$ = unit normal); and $dW_B(\mathbf{ds})$ is the surface energy associated with crack growth $\mathbf{ds}$.

For homogeneous materials, the surface $\mathbf{ds}$, in equation (1), is well defined and the direction dependency of fracture energy refers only to the possible anisotropy of the material. But for heterogeneous materials the area increment of the extending fissure remains ill-defined. Indeed, as shown by Hoagland, et al., [5], when tensile ruptures develop in rocks, a zone of intense microcracking may propagate ahead of the macroscopic fissure. As a consequence the area of the newly created discontinuities may not coincide with that of the macroscopic fissure increment.

In order to overcome this difficulty, the quantity of energy absorbed by the microscopic process may be included conveniently in the definition of γ in equation (2) and the fissure increment area is defined then as the area of the actual macroscopic fissure increment. But this microcracking process depends on the stress gradient ahead of the fissure so that the extent of the zone affected by this phenomenon is
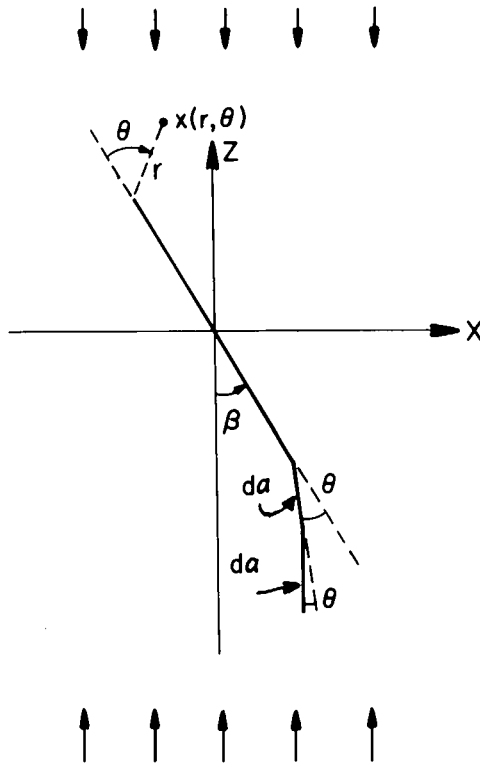
Fig. 1 Coordinate system

not an intrinsic rock characteristic. It follows that proper derivation of equation (2) for rock, not only must include any possible anisotropic influence, but also must take into account the stress gradient effect.

For quasi-static, adiabatic, fracturing processes the crack configuration which corresponds to a small area increment da must satisfy

$$[\Delta W_E(X) - \Delta W_B(X)] - [\Delta W_E(X_0) - \Delta W_B(X_0)] < 0 \qquad (3)$$

where $\Delta W_E(X)$ is the strain-energy release associated with any virtual crack increment configuration X, the configuration X_0 corresponding to the actual extended crack; $\Delta W_B(X)$ represents the quantity of surface energy absorbed by the crack extension implied by configuration X.

If, as the crack extends the quantity $(\Delta W_E(X_0) - \Delta W_B(X_0))$ increases while the far-field stress state is maintained constant, fracture is unstable.

A two-dimensional analysis is proposed (plane strain deformation of a slice of unit thickness) so that a crack increment is characterized by its area $da = dl \times 1$ and its orientation θ with respect to the previous crack increment (see Fig. 1).

Equation (3) represents the strain-energy release-rate criterion of fracture for adiabatic, quasi-static conditions; it is similar in its concept to the criteria proposed by Palaniswamy and Knauss [6] and Nuismer [7].

An alternative energy criterion has been proposed by Sih [3] on the hypothesis that a crack spreads in the direction of maximum potential energy density, that is the direction along which the strain-energy density is a minimum, and that the critical intensity of this potential field governs the onset of crack propagation.

In a two-dimensional analysis, if r and θ are the coordinates of a point near the tip of an elliptical crack (Fig. 1), it can be shown [2], that stress components present a singularity in $r^{-1/2}$ so that the strain-energy density is singular in $1/r$; this last quantity can be expressed in terms of Irwin's stress-intensity factors [2], for sufficiently small r, as follows:

$$\frac{dW_E}{dV} = \frac{1}{r}(a_{11}k_1{}^2 + a_{12}k_1k_2 + a_{22}k_2{}^2 + a_{33}k_3{}^2) \qquad (4)$$

where k_1, k_2, k_3 are the stress-intensity factors for cracks deformations in modes I, II, and III.

a_{ij} are parameters which depend only on the elastic characteristics of the material and on the angle θ.

Sih [3] defined the strain-energy-density factor as the quantity

$$S = \frac{dW_E}{dV} \cdot r \qquad (5)$$

for representing the intensity of the strain-energy-density field. S varies with the angle θ and the direction θ_0 along which the crack extends is such that

$$\left.\frac{\partial S}{\partial \theta}\right|_{\theta=\theta_0} = 0, \qquad \left.\frac{\partial^2 S}{\partial \theta^2}\right|_{\theta=\theta_0} > 0 \qquad (6)$$

Equation (6) represents the strain-energy-density factor theory. If S decreases as the crack extends while the far-fields stress state is maintained constant, the fracturing process is considered stable.

The Numerical Model

For stress-free cracks, exact solutions for the strain-energy release rate as well as for the strain-energy-density factor have been obtained, e.g., [2, 3, 8]. However no closed-form solution exists yet to the problem of cracks propagating in directions other than their own initial orientation and for which frictional resistance caused by crack closure develops.

The only presently feasible approach requires the use of a numerical technique. The displacement-discontinuity method seems well suited to solving this kind of problem.

The Displacement-Discontinuity Method. In recent publications, e.g., [9, 10] it has been proposed to analyze crack problems by the integral equation formulation method. This method is based on the numerical solution of a set of integral equations which relate boundary displacements and boundary tractions through the use of a singular solution (usually Kelvin's solution for a point force in the interior of an infinite elastic solid) to develop a Green's function type of relationship for the boundary values. This technique reduces the problem dismensionality by one and implies discretization only along the boundaries of the domain under consideration as opposed to the finite differences techniques which necessitate that the entire domain be discretized.

The displacement-discontinuity technique, described by Crouch and chosen for the present study, is similar to the integral equation method in that it is based on the use of influence functions to produce a system of simultaneous equations involving only boundary conditions. But with this approach the singularities are taken care of algebraically in the analytic solution; the finite displacement of a segment referred to as a "displacement-discontinuity" replaces the infinite displacement of the point solution.

For plane strain conditions the displacements are expressed with the classical Neuber/Papkovitch representation [11].

$$U_x = B_x - \frac{1}{4}(1 - \nu) \cdot \partial/\partial x(xB_x + zB_z + \beta)$$

$$U_z = B_z - \frac{1}{4}(1 - \nu) \cdot \partial/\partial z(xB_x + zB_z + \beta) \qquad (7)$$

where U_x and U_z are the x and z-components of the displacements at point $X(x, z)$ and B_x, B_z, and β are functions in x and z.

Two particular sets of functions are derived; the first one corresponds to an infinite body with the plane $z = 0$ free from normal tractions and the second one to the same body with the plane $z = 0$ free from shear tractions. Exact solutions for the stresses and displacements in an infinite, or semi-infinite, medium caused by a constant displacement along a line segment are then determined. Finally, these solutions are taken singly or combined to construct solutions to boundary-value problems. This provides a set of linear equations relating boundary stresses and boundary displacements to a set of displacement-discontinuities $\hat{u}$ placed along the boundary of the domain under consideration.

The normal and tangential stresses acting at the center of a segment of the boundary are related to the displacement-discontinuities $\hat{u}$'s of all segments by

$$\begin{Bmatrix} \sigma_t \\ \sigma_n \end{Bmatrix} = \begin{bmatrix} A_{tt} & A_{tn} \\ A_{nt} & A_{nn} \end{bmatrix} \begin{Bmatrix} \hat{u}_t \\ \hat{u}_n \end{Bmatrix} \qquad (8)$$

where the A's are N by N submatrices and σ_t, σ_n, $\hat{u}_n$, and $\hat{u}_t$ are column vectors of N components (for N displacement-discontinuities).

The tangential and normal components of the displacements are related to the displacement-discontinuities by a similar set of equations

$$\begin{Bmatrix} U_t \\ U_n \end{Bmatrix} = \begin{bmatrix} B_{tt} & B_{tn} \\ B_{nt} & B_{nn} \end{bmatrix} \begin{Bmatrix} \hat{u}_t \\ \hat{u}_n \end{Bmatrix} \qquad (9)$$

where the B's are N by N submatrices and U_t and U_n are column vectors of N components.

The coefficients A's and B's depend solely on the geometry of the problem and on the material properties. If an additional discontinuity is introduced, only one line and one column have to be added to the previous submatrices; all the other coefficients remain unchanged.

Once the coordinates and the boundary conditions of the N displacement-discontinuities have been defined, the system of N equations can be solved for the unknown displacements $\hat{u}$'s. The stress state and the displacements at any point of the continuum are then obtained directly from equation (8) or (9); this time however the $\hat{u}$'s are known and the σ's and U's are computed.

Because the displacements are constant throughout each boundary segment, it is necessary to introduce more discontinuities in regions of high strain than in those of uniform deformation. In addition, because the average stresses at each discontinuity location is supposed to be that of segment midpoint, some error in the stress determination may occur. This shortcoming could be improved by use of "influence coefficients" to average the stress field within a distance of each segment end points.

Since the material is assumed to be linearly elastic it is possible to superpose a free stress field to the boundary stresses so that, for example, given constant stress conditions be defined at infinity.

The variation of strain energy which results from the prescribed boundary conditions is obtained by direct application of Clapeyron's strain-energy theorem [12] which states that when a body is in equilibrium, the strain energy of the deformation is equal to one half of the work that would be done by the external forces (at the equilibrium state) acting through the displacements from the unstressed state to the state of equilibrium.

Crack Propagation Analysis. A fissure, or crack, is represented in this model by a set of displacement-discontinuities the lengths of which are adjusted to the displacement gradient so that the discretization process remains representative of the problem. The surfaces of these elements are allowed either to become separated or to slide against one another but no interpenetration is allowed (normal displacements cannot be positive). In the case of sliding, the frictional resistance to shear displacements is directly proportional to the applied normal force; if the frictional force is larger than the tangential force which exists before any displacement occurs, sliding is precluded and, in this particular case, there is no discontinuity in the displacement field along the corresponding segment.

The crack path derived from the maximum strain-energy release-rate hypothesis implies that the linear system which defines the $\hat{u}$'s be solved for each virtual crack configuration. The strain-energy variations associated with various virtual crack extension configurations is computed and that which provides the largest strain-energy release is chosen as crack path (see equation (3)). Clearly when the quantity $\Delta W_E(\theta, dl)$ is computed, care must be taken about what length to choose for dl.

This is done numerically by requiring that

$$\left[\Delta W_E(\theta, dl)/dl - \Delta W_E\left(\theta, \frac{dl}{2}\right) \Big/ \frac{dl}{2} \right] < \epsilon \qquad (10)$$

where ϵ reflects the degree of accuracy chosen for the analysis.

The strain-energy-density factor is determined by direct computation

$$S = [(1 - \nu)(\sigma_{11}{}^2 + \sigma_{22}{}^2) - 2\nu\sigma_{11}\sigma_{22} + \sigma_{12}{}^2](1 + \nu)r/E \qquad (11)$$

It must be noted that the displacement-discontinuity technique is inaccurate for points in the immediate neighborhood of the tip of the last discontinuity of the crack. Accordingly it is essential to have sufficiently small elements at the crack tip so that the domain D_1, for which the numerical technique becomes inaccurate be smaller than the domain D_2 for which the strain-energy density can be approximated by a function in $1/r$.

Ingraffea [13] proposed to determine the strain-energy-density factor from the stress-intensity factors through the use of equation (4); the stress intensity factors, in turn, were computed from the displacements near the crack tip (COD technique used in finite-element analysis). This technique has not been followed here for it is not clear whether equation (4) derived for linear cracks is still applicable to curved cracks, especially in regard of the influence of the nonsingular terms for the near crack tip stress field. It is recognized however that some inaccuracy may occur because of the direct computation involving squares of computed stresses. This is discussed in light of the illustrative examples described hereafter.

Also, the change in stress field caused by the change in crack configuration should take into account the crack configuration history since the problem is geometrically nonlinear. Indeed, the influence of frictional resistance should be taken into account for the loading process as well as for the local unloadings caused by the change in crack configuration. The influence of this geometrical nonlinearity has been assumed negligible with regard to the qualitative discussion proposed hereafter. Once again, although the present model can be used to determine the loading conditions for which a crack extends, the main purpose of this paper is to describe a numerical model easily applicable to the determination of crack path. Current work is oriented to solving this nonlinearity problem by determining the stress field related to the $(n + 1)$th crack configuration with the following initial conditions:

1 Original far-field stress state (this one is supposed to remain constant throughout crack propagation).

2 Crack in the deformed position reached at the nth configuration with corresponding shear stress distribution on the crack surfaces.

3 $(n + 1)$th crack increment free from any shear stress.

Practical Examples

Uniaxial Tensile Stress Field at Infinity. *Crack Perpendicular to the Stress Field at Infinity.* This example has often been analyzed and the exact solution for the strain-energy release rate G and the strain-energy-density factor S, are known; e.g., [2, 3, 8]. Numerical results for G at $\theta = 0°$ (see Fig. 1) are found to depend only on the crack increment length. If a is the half crack length and da its increment, for $da/a = 0.02$ error was 0.8 percent, for $da/a = 0.006$ error was 0.3 percent.

The model indicates that the crack propagates in its own direction in an unstable manner. Thirteen different crack orientations were investigated $(-90° < \theta < +90°)$; the total computer time used for 3 crack increments was less than 20 sec on a Control Data Cyber 74 computer for 22 discontinuities distributed along the half-crack length (symmetry was taken advantage of).

Similar conclusions are reached with the critical strain-energy-density-factor hypothesis. However the accuracy on S depends strongly upon the boundary segments pattern used to simulate the crack (see Fig. 2).

Crack Oriented at 45° With Respect to the Applied Stress Field. It was found that G (the strain-energy release rate) exhibits a maximum value for $\theta = 48.7°$ (the angle increments $d\theta$ used in the numerical differenciation were equal to $3.75°$) and, according to equation (3), the crack should extend in this direction.

When considering the variation of S (the strain-energy-density factor) with respect to θ, it is found that S does present a stationary value for $\theta = 48.7°$ and that this value corresponds to the largest relative minimum, as required by Sih's theory.

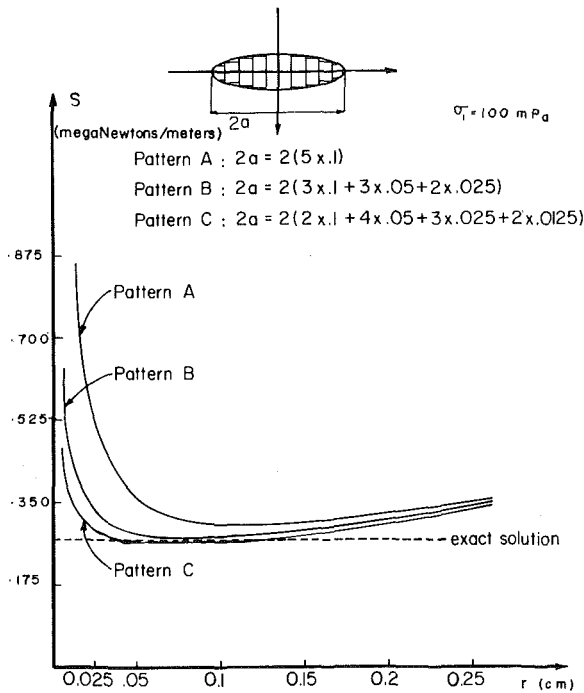If the crack is discretized in 150 elements, the numerical model gives

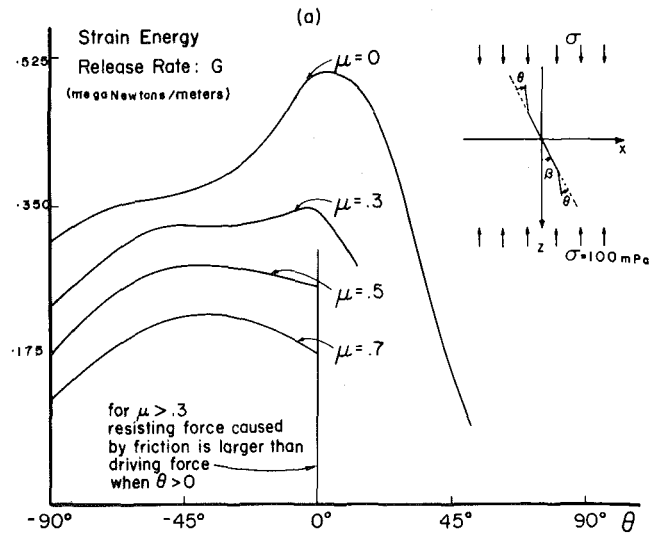**Fig. 2** Variation of the strain-energy-density factor with discontinuities pattern

Fig. 3(a) Influence of the friction coefficient μ on the strain-energy release-rate variation for a crack inclined at 30° with respect to a uniaxial compressive stress
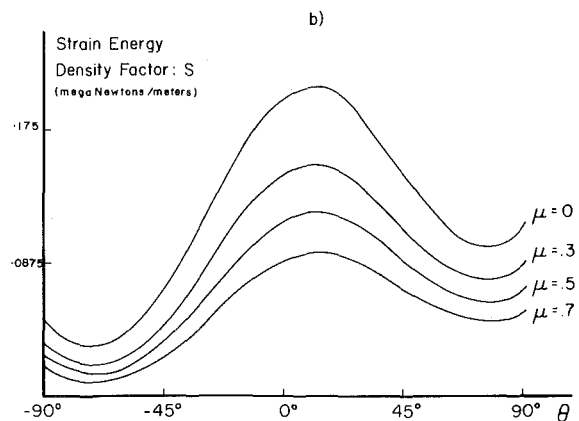

Fig. 3(b) Influence of the friction coefficient μ on the strain-energy-density factor in the vicinity of the tip of a crack inclined at 30° with respect to a uniaxial compressive stress field

values for S within 5 percent of those derived with the classical series expansion developed for elliptical crack tips [3], computed at $r = 0.01$ cm for crack length $2a = 1$ cm.

It may be worth pointing out that the θ-value for which S reaches its largest relative minimum was found to be correct with a 30 discretization elements pattern but the corresponding value computed for S was erroneous by about 16 percent.

Compressive Stress Fields at Infinity. Numerical investigations of crack propagation in compressive stress fields, based on an energy criterion of fracture, have been reported previously in the literature; e.g., [13–15]. Yet in these analysis, crack surfaces remain stress-free, a hypothesis which is not always realistic for line cracks submitted to compressive stress fields, since crack closure does occur.

Uniaxial Compression. Values for G (the strain-energy release rate) were computed for a line crack inclined at $\beta = 30°$ with respect to the direction of the applied load with crack increments of constant length dl but variable orientation θ (Fig. 3(a)). Similarly values for S (the strain-energy-density factor) were derived for the same crack tip (constant r, variable θ, see Fig. 3(b)).

The influence of crack increment length on the computed value for G has been investigated numerically. With equation (12) as a criterion of convergence, it was found that a relative crack increment $da/a = 0.002$ (a = half-crack length) provided a relative error on G/a smaller than 5 percent. Although the computed value for G as obtained with crack increments such that $da/a = 0.0125$ differed by 15 percent from that obtained with crack increments such that $da/a = 0.0032$, the difference in crack path was negligible for all practical purposes except at the very tip of the original fracture. For this analysis it is necessary to insure that crack increment length is compatible with the discretization pattern near the crack tip.

Angular variations of G were investigated for $-90° < \theta < 90°$ at angular steps $\Delta\theta$. For $\Delta\theta = 7.5°$, the determination of three incremental crack length (such that $da/a = 0.001$) required nine minutes with an IBM 370-168 computer. In fact this time depends greatly on the amount of elements used to discretize the crack and on the amount of virtual crack increment orientations which are considered. For crack increment length such that $da/a = 0.0062$ and orientations changing from $-15°$ to $+75°$, the same computation can be conducted in less than two minutes.

A few conclusions can be derived from this investigation. First of all, the results for S, as obtained with the numerical model, are significantly different from those derived from the stress-free elliptical crack tip solution [3, 5].

Second, the crack increment orientation for which G reaches a maximum depends on the magnitude of the friction coefficient μ while the orientation θ for which S exhibits stationary values remains unchanged as μ varies.

In addition, the largest relative minimum for S occurs for positive values of θ while the maximum for G is reached for negative θ, domain in which S reaches an absolute minimum; the value of θ for this absolute minimum is different from that for G maximum.

Further the numerical results indicate that the strain-energy release rate computed for the straight line crack is directly proportional to crack length, a feature which is similar to that obtained analytically for penny-shaped cracks submitted to either tensile or compressive uniaxial stress fields.

Finally, with the G criterion the crack extension process was found to be stable with respect to applied stresses, except for the case of zero friction coefficient.

Triaxial Compression. The angular increments used in the numerical differentiation were fairly large (15°) for the only purpose of
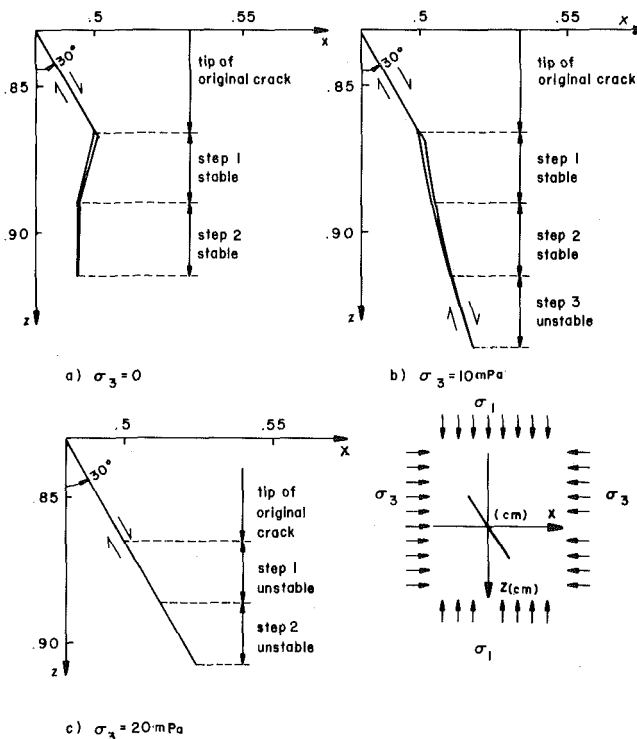
Fig. 4 Crack path predicted by the strain-energy release-rate criterion for triaxial compressive stress fields; ($\sigma = 100$ mPa for (a, b and c))

the analysis was to investigate general trends of fracture development and not to obtain practical results for a specific material.

With the maximum G criterion it was found that, for low values of σ_3(σ_1 is the largest principal stress and σ_2 is defined by the plane strain conditions; compressive stresses being taken positive). Cracks of various orientation β initially propagate in a stable manner toward a fixed direction θ_c; in this process the crack increment surfaces are not in contact. This suggests that crack propagation can be interpreted as a superposition of fractures by mode I and II as defined by Irwin [2]. Once the cracks are oriented along this critical direction θ_c, extension continues with the same orientation in an unstable manner without any crack opening (only sliding along the crack surface occurs).[1] Fig. 4 indicates the variations of θ_c with the magnitude of σ_3. In addition it was found that with the maximum G hypothesis, as the value of σ_3 increases, the extent of the crack portion which opens decreases and even vanishes for a ratio σ_1/σ_3 smaller than 4. When the value for σ_3 becomes too large (σ_1/σ_3 smaller than 3.3) the model does not apply any longer because the frictional resistance for all crack orientations becomes larger than the shearing force for the 0.5 friction coefficient chosen in this analysis.

If the absolute minimum S criterion is used, meaningless results are obtained (after a few incremental steps the crack intersects itself, see Fig. 5(a)).

This is similar, although within a slightly different context, to Ingraffea's finding [13]. Ingraffea proposed modification to Sih's criterion in that fracture should extend in the direction along which S is minimal over those values of θ (see Fig. 1) for which the mode I stress-intensity factor $k_\mathrm{I}(\theta)$ is positive.

In the present paper a somewhat similar approach has been followed but stress concentration factors have been considered instead of stress-intensity factors: crack paths have been computed so that they follow the direction for which S is minimum and for which the

minimum principal stress is smallest (compressive stresses were taken positive).

With this criterion, for the 100 bars confining pressure example, the first crack increment occurs in the direction for which $S(\theta)$ reaches its absolute minimum value while all other orientations correspond to the largest relative minimum. The crack extends in mixed mode I and mode II so that the extended crack is "opened" (see Fig. 5(b)). For the $300b$ confining pressure example, the crack is found to propagate in sawteeth (any new crack increment is parallel to the one before last) so that only average direction trend can be defined. All orientations correspond to absolute minimum values for $S(\theta)$; no crack opening is noticed (crack propagates monotonically in a compressive stress field).

For the $100b$ case, the magnitude of S decreases with crack extension, a feature which would suggest that the crack stabilizes after a few increments; for the $300b$ case, the opposite is observed.

Finally, crack propagation directions are found to depend on the magnitude of σ_3 (if σ_1 is kept constant). After 5 increments of length equal to 0.025 cm for an original crack length of 1 cm, all paths are found to be inclined with respect to the major principal stress direction at an angle the sign of which is opposite to that of the original crack orientation β (see Fig. 1).

Discussion and Conclusion

This analysis has been restricted to the problem of quasi-static propagation of cracks in homogeneous isotropic linearly elastic solids subjected to plane strain conditions.

For these conditions, the numerical model derived from the displacement-discontinuity technique has been shown to be well suited for investigating strain-energy variations caused by crack propagation as well as changes of strain-energy density in the neighborhood of a crack tip. Results obtained with the model for a crack perpendicular to a uniaxial tensile stress field were found to be within 0.3 percent of analytical solutions for the strain-energy release rate (G) and 1 percent for the strain-energy-density factor (S). For cracks inclined at a 45° angle with respect to the uniaxial tensile stress field, the strain-energy-density factor computation was within 5 percent of the closed-form solution. Although an accurate computation of S magnitude requires a large number of elements (150 for a 5 percent accuracy), directions for which S reaches minimum values are determined with accuracy with far less elements (30 was found sufficients for the inclined crack).

For tensile stress fields, the maximum strain-energy release-rate criterion and the critical strain-energy-density-factor criterion gave similar results for the crack path and for the fracturing process stability.

For compressive stress fields, in which the crack closes so that its surface comes into contact and slides against one another, the results derived from the two criterion with the numerical model differed significantly.

Values for S as obtained with the model were mentioned to differ from those published for frictionless cracks; but this difference results from the mathematical representation of the crack. In the model, when the crack closes it is assimilated to a discontinuity in the displacement field only for the direction along the crack, while for the elliptical crack tip model, the radius of curvature at the tip of the crack remains always finite. It is not clear which configuration is closer to reality and in order to compare results obtained with the G and S criteria the same crack modeling must be adopted for both derivations.

The main differences observed with the two criteria are as follows:

1 The largest relative minimum for S was associated to positive angles θ while the maximum value of G was obtained for negative θ.

2 The negative θ-value for which S reached a minimum did not coincide with that for which G was maximum.

3 The critical strain-energy-density-factor hypothesis showed that fracture mode is unaffected by the friction coefficient magnitude;
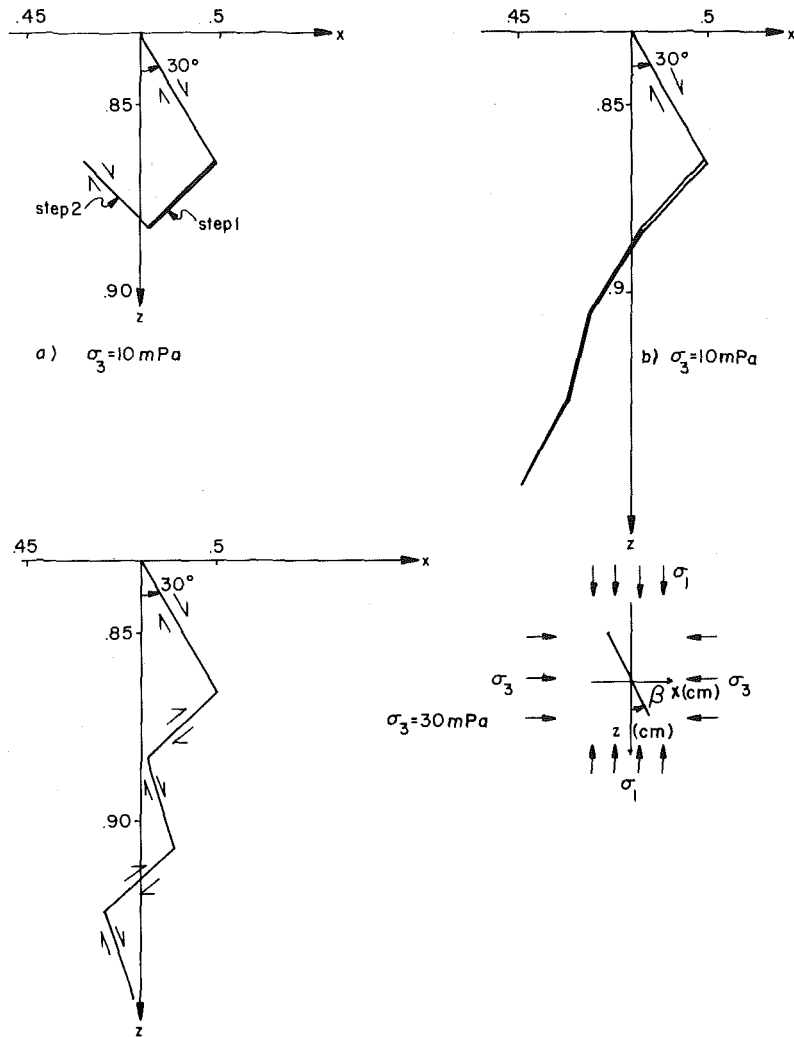
---

[1] When $\sigma_3 = 0$, the crack propagates toward the direction of σ_1 and remains stable.

Fig. 5   Crack path predicted by the strain-energy-density factor criterion for triaxial compressive stress fields; (σ_1 = 100 mPa for all cases)

the opposite result was observed with the maximum strain-energy release-rate criterion.

4   For triaxial conditions, both criteria indicate that the crack path depends on the ratio σ_1/σ_3. With the G criterion, decreasing this ratio value results in favoring shear mode propagation over tensile mode; also, as σ_3 increases, the crack path tends toward a direction which is inclined with respects to the major principal stress direction at an angle of similar sign to that of the original crack orientation. A similar result is obtained, except for the crack path angle, with the S criterion, if it is modified so as to consider the relative minimum of S for which the stress concentration factor of the least principal stress is smallest.

Although no experimental figures are available to verify quantitatively which path configuration is closest to reality, the following can be said:

1   Experiments on glass samples by Hoek and Bienawski [16] indicate that crack propagation occurs for negative values of θ. This experimental observation is in agreement with results derived with the G criterion but not with those derived from the largest relative minimum S criterion.

2   If one retains constantly the crack path associated with the absolute minimum for S, the crack is found to intersect itself, a feature which is not experimentally acceptable.

For triaxial loading conditions, except for Hoek and Bienawski's experimental results in which, from the very author's point of view,

sliding was precluded, the overall scheme for rock samples failure is always the same, e.g., [17–19]:

1   Large dilantacy associated with vertical splitting is obtained for uniaxial load conditions. The fracturing process is stable in the sense that, with very stiff testing machine, work has to be performed continuously on samples to reach complete failure.

2   Fracture along a single plane inclined with respect to the maximum principal stress direction arises for triaxial stress conditions ($\sigma_2 = \sigma_3$ = confining pressure). The angle between the fracture plane and the maximum principal stress depends on the confining pressure magnitude. Some dilatancy is observed before complete failure is attained the amount of which decreases as the confining pressure is increased. The fracturing process is unstable in the sense that the specimen must be unloaded if fracture is to be controlled.

These experimental macroscopic features compare fairly well with those obtained with the numerical model and the maximum strain energy release rate criterion.

The numerical results, derived with the modified critical strain-energy-density factor, for the overall crack path orientation do not seem to agree as well, phenomenologically, with the experimental shear fracturing process.

Acknowledgments

program available. May he, along with Professor Sih, Dr. T. P. Bligh, and Dr. J. K. Daemen find here the expression of my sincere gratitude for their helpful criticisms and comments. However I bear the entire responsibility for the views expressed here; IPG contribution 328.

References

1 Griffith, A. A., *Philosophical Transactions of the Royal Society*, London, Series A, Vol. 221, 1921, p. 163.

2 Irwin, G. R., ASME JOURNAL OF APPLIED MECHANICS, Vol. 24, 1957, pp. 361–364.

3 Sih, G. C., *Mechanics of Fracture*, Vol. 1, Noordhoff International Publishing, Leyden, The Netherlands, 1973, XXI–XLV.

4 Crouch, S. L., *International Journal of Numerical Methods in Engineering*, Vol. 10, 1976, pp. 301–343.

5 Hoagland, R. G., et al., ARPA Research Contract M021006, U.S. Bureau of Mines, Twin Cities, U.S.A., 1972.

6 Palaniswami, K., and Knauss, W. G., California Institute of Technology Graduate Aeronautical Laboratories, Report SM 74-8, 1974, pp. 4–9.

7 Nuismer, R. J., *International Journal of Fracture*, Vol. 11, 1975, pp. 245–251.

8 Rice, J. R., *Fracture*, Vol. 2, ed., Liebowitz, Academic Press, New York, 1968, pp. 169–311.

9 Cruse, T. A., *Computers and Structures*, Vol. 3, 1973, pp. 509–527.

10 Snyder, M. D., and Cruse, T. A., *International Journal of Fracture*, 1975, pp. 315–328.

11 Timoshenko, S. P., and Goodyear, J. N., *Theory of Elasticity*, 3rd ed., McGraw-Hill, New York, 2nd ed., 1970, p. 242.

12 Sokolnikof, I. S., *Mathematical Theory of Elasticity*, McGraw-Hill, New York, 2nd. ed., 1956, p. 86.

13 Ingraffea, A. R., PhD thesis, The University of Colorado, Department of Civil, Environmental, and Architectural Engineering, 1977.

14 Miyamoto, H., Fukuoa, S., and Kageyama, K., *Proceedings, Congress on Fracture, IV*, Vol. 3, 1977, pp. 491–499.

15 Kipp, M. E., and Sih, G. C., *International Journal of Solids and Structures*, Vol. 11 n°2, 1975, pp. 153–173.

16 Hoek, E., and Bienawski, Z. T., *International Journal of Fracture Mechanics*, Vol. 1, 1965, p. 137.

17 Griggs, D. T., *Journal of Geology*, Vol. 44, 1936, pp. 541–577.

18 Handin, J. H., and Hager, R. V., *Bulletin of the American Association of Petroleum Geologists*, Vol. 41, 1957, pp. 1–50.

19 Cornet, F. H., and Fairhurst, C., *Percolation Through Fissured Rocks*, Symposium of the International Society for Rock Mechanics, 1972, p. 12-A.